View metadata, citation and similar papers at core.ac.uk
brought to you by CORE
provided by Illinois Digital Environment for Access to Learning and Scholarship Repository

In situ poly(urea-formaldehyde) microencapsulation of dicyclopentadiene*

E. N. BROWN[1,2], M. R. KESSLER[3], N. R. SOTTOS[1,2], and S. R. WHITE[4,2]

[1]Department of Theoretical and Applied Mechanics
University of Illinois at Urbana-Champaign, Urbana, IL, 61801
[2]Beckman Institute for Advanced Science and Technology
University of Illinois at Urbana-Champaign, Urbana, IL, 61801
[3]Department of Mechanical Engineering
The University of Tulsa, Tulsa, OK, 74104
[4]Department of Aeronautical & Astronautical Engineering
University of Illinois at Urbana-Champaign, Urbana, IL, 61801

Abstract

Microencapsulated healing agents that possess adequate strength, long shelf-life, and excellent bonding to the host material are required for self-healing materials. Urea-formaldehyde microcapsules containing dicyclopentadiene were prepared by *in situ* polymerization in an oil-in-water emulsion that meet these requirements for self-healing epoxy. Microcapsules of 10-1000 μm in diameter were produced by appropriate selection of agitation rate in the range of 200-2000 rpm. A linear relation exists between log(mean diameter) and log(agitation rate). Surface morphology and shell wall thickness were investigated by optical and electron microscopy. Microcapsules are composed of a smooth 160-220 nm inner membrane and a rough, porous outer surface of agglomerated urea-formaldehyde nanoparticles. Surface morphology is influenced by pH of the reacting emulsion and interfacial surface area at the core-water interface. High yields (80-90%) of a free flowing powder of spherical microcapsules were produced with a fill content of 83-92 wt% as determined by CHN analysis.

Keywords: microcapsule, self-healing, dicyclopentadiene, urea formaldehyde, *in situ* polymerization, surface morphology

---

* Submitted for publication in *Journal of Microencapsulation* (2003)

Introduction

Self-healing polymers and composites with microencapsulated healing agents offer tremendous potential for providing long-lived structural materials (White *et al.* 2001). The microcapsules in self-healing polymers not only store the healing agent during quiescent states, but provide a mechanical trigger for the self-healing process when damage occurs in the host material and the capsules rupture. The key feature of self-healing materials is the highly engineered microencapsulated healing agent. The microcapsules must possess sufficient strength to remain intact during processing of the host polymer, yet rupture when the polymer is damaged. High bond strength to the host polymer combined with a moderate strength microcapsule shell are required. To provide long shelf-life the capsules must be impervious to leakage and diffusion of the encapsulated (liquid) healing agent for considerable time. These combined characteristics are achieved with a system based on the *in situ* polymerization of urea-formaldehyde (UF) microcapsules encapsulating dicyclopentadiene (DCPD) healing agent, outlined in Figure 1. The addition of these microcapsules to an epoxy matrix also provides a unique toughening mechanism for the composite system (Brown *et al.* 2002).

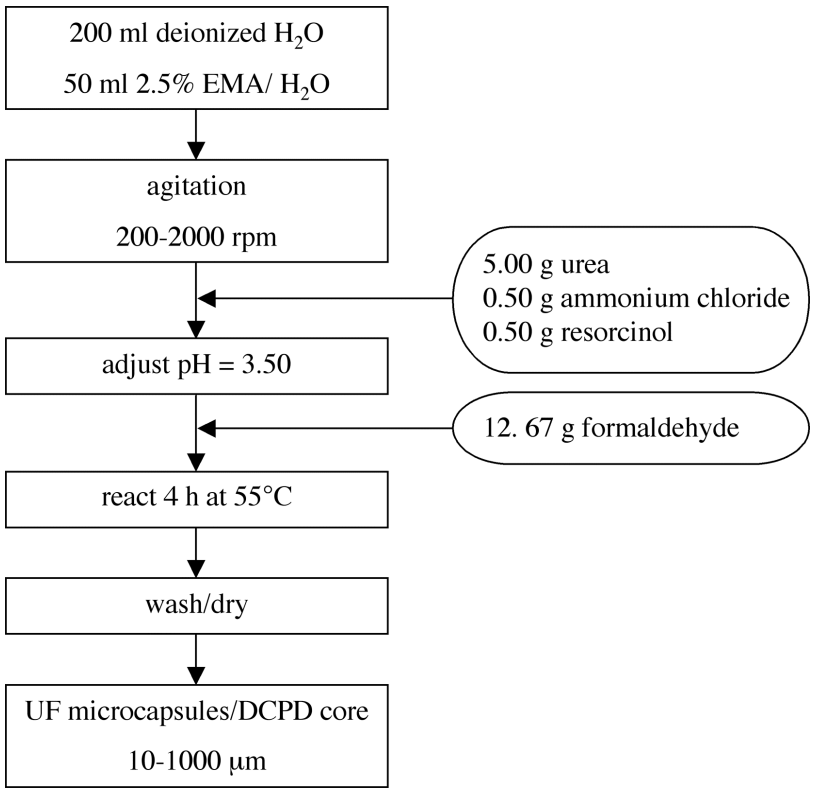

Figure 1. Microencapsulation of DCPD utilizing acid-catalyzed *in situ* polymerization of urea with formaldehyde to form capsule wall.

Here we report on the manufacture of UF microcapsules prepared by *in situ* polymerization in an oil-in-water emulsion. A basic review of the *in situ* encapsulation technique has been provided by Baxter (1974), Thies (1987, 1996), and Arshady and George (1993). *In situ* encapsulation of water-immiscible liquids by the reaction of urea with formaldehyde at acid pH is outlined by Dietrich *et al*. (1989). Tan *et al*. (1991), Yan *et al*. (1993), Alexandridou and Kiparissides (1994), and Ovez *et al*. (1997) have all shown that microcapsule size can be controlled by adjusting the agitation rate during microencapsulation.

UF microcapsule diameter and surface morphology significantly influence capsule rupture behavior and healing agent release in self-healing polymers (White *et al*. 2001, Brown *et al*. 2002). In this paper UF encapsulated DCPD with average diameter ranging from 10 to 1000 μm are analyzed and the influence of process variables on the capsule surface morphology is described.

Materials and methods

Materials

Dicyclopentadiene was obtained from Acros Organics (Geel, Belgium) and purified by filtration and vacuum distillation prior to microencapsulation. Urea, ammonium chloride, and formaldehyde were purchased from Fisher Chemicals (Loughborough, UK). Resorcinol was obtained from J. T. Baker (Phillipsburg, New Jersey). Ethylene maleic anhydride (EMA) copolymer was purchased from Zeeland Chemicals (Zeeland, Michigan). All solvents and substances used for preparation of EMA solution, acid and base solutions and 1-octanol were of analytical grade.

Preparation of microcapsules

Microcapsules were prepared by *in situ* polymerization in an oil-in-water emulsion. At room temperature (20-24°C) 200 ml of deionized water and 50 ml of 2.5 wt% aqueous solution of EMA copolymer were mixed in a 1000 ml beaker. The beaker was suspended in a temperature-controlled water bath on a programmable hotplate with external temperature probe (Dataplate® Digital Hotplate, Cole Palmer). The solution was agitated with a digital mixer (Eurostar, IKA Labortechnik) driving a three-bladed, 63.5 mm diameter low-shear mixing propeller (Cole Parmer) placed just above the bottom of the beaker.

Under agitation, 5.00 g urea, 0.50 g ammonium chloride, and 0.50 g resorcinol were dissolved in the solution. The pH was raised from approximately 2.60 to 3.50 by drop-wise addition of sodium hydroxide (NaOH) and hydrochloric acid (HCl). One to two drops of 1-octanol were added to eliminate surface bubbles. A slow stream of 60 ml of DCPD was added to form an emulsion and allowed to stabilize for 10 minutes. After

stabilization, 12.67 g of 37 wt% aqueous solution of formaldehyde was added to obtain a 1:1.9 molar ratio of formaldehyde to urea (Sanghvi and Nairn 1992). The emulsion was covered and heated at a rate of 1°C min^{-1} to the target temperature of 55°C. After four hours of continuous agitation the mixer and hot plate were switched off. Once cooled to ambient temperature, the suspension of microcapsules was separated under vacuum with a coarse-fritted filter. The microcapsules were rinsed with deionized water and air dried for 24-48 h. A sieve was used to aid in separation of the microcapsules (U.S.A. standard testing sieves, W. S. Tyler).

Microcapsule size analysis

Microcapsule size analysis was performed with an optical microscope (Optiphot 150S, Nikon) and image analysis software (Global Lab Image V. 3.1, Data Translation). Mean diameter and standard deviation were determined from data sets of at least 250 measurements. The size distribution was biased toward small microcapsule diameters as discussed by Ovez *et al*. (1997), however the mean and standard deviation captured the dominant mode of the distribution.

Electron microscopy

Surface morphology and capsule shell thickness were examined by scanning electron microscopy (XL30 ESEM-FEG, Philips). Microcapsules were mounted on a conductive stage and ruptured with a razor blade to facilitate membrane thickness measurement. Samples were sputtered with a thin layer (~10 nm) of gold-palladium to prevent charging under the electron beam.

Elemental analysis

Microcapsule fill content was measured by elemental analysis using a Carbon-Hydrogen-Nitrogen (CHN) analyzer (CE440, Exeter Analytical Inc.). Microcapsules samples combusted at 980°C in an oxygen atmosphere to form CO_2, H_2O, and N_xO_y. Knowing the chemical compositions of UF ($C_5H_8N_2O$, 53.56 wt% C and 24.98 wt% N) and DCPD ($C_{10}H_{12}$, 90.85 wt% C and 0 wt% N), and assuming that water was the only impurity present in the combusted sample, the weight fractions of UF and DCPD were calculated as

$$\begin{aligned} w_{\mathrm{UF}} &= 4.003 w_{\mathrm{N}} \\ w_{\mathrm{DCPD}} &= 1.101 w_{\mathrm{C}} - 2.144 w_{\mathrm{N}} \end{aligned} \tag{1}$$

where w_{C} and w_{N} are the weight fractions of C and N obtained by elemental analysis.

Results and discussion

The processing route described in Figure 1 produces high quality UF microcapsules with a DCPD core over a wide range of sizes for use in self-healing structural polymers and polymer composites. The microcapsules are spherical and free flowing after drying (see Figure 2). Yields of the preparation, defined by the ratio of the mass of recovered microcapsules to the total mass of DCPD core and shell constituents, are high. At 550 rpm agitation rate the typical yield is 79-92%. Fracture of microcapsules under high shear conditions and nonrecoverable microcapsule buildup on the reaction beaker result in lower yields as agitation rate increases. At 1800 rpm agitation rate, the typical yield is greater than 68%.

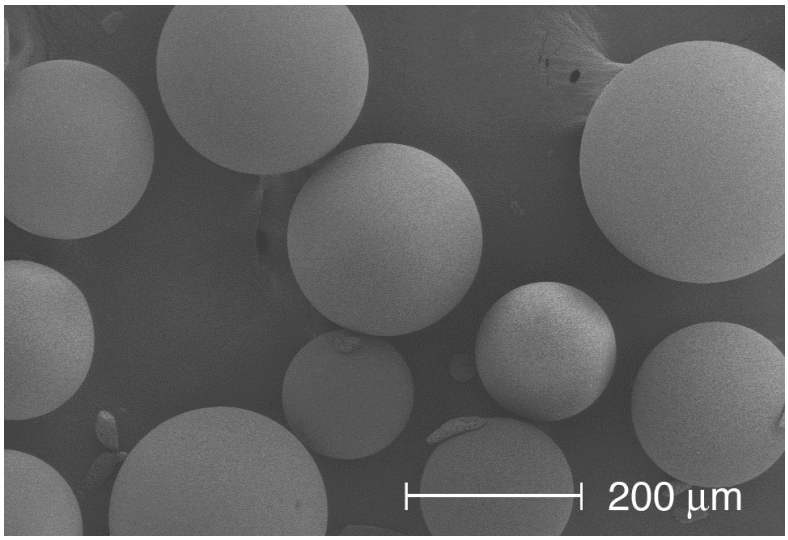

Figure 2. ESEM image of UF microcapsules containing DCPD core. The microcapsules were prepared following the procedure in Fig. 1 at 550 rpm agitation rate.

Control of diameter

Average microcapsule diameter is controlled by agitation rate as shown in Figure 3. As the agitation rate is increased, a finer emulsion is obtained, and the average microcapsule diameter decreases. Microcapsules with average diameter in the range of 10-1000 μm are obtained by adjusting agitation rate between 200–2000 rpm. The standard deviation is less than 35% of the mean value over the entire range of diameters produced. Over the agitation rates investigated the relationship between average diameter and agitation rate is linear in log-log scale, as is the dependence between droplet size and shear rate as described by Taylor (1932). Although a logical correlation exists between agitation rate and shear rate, the connection to Taylor's work is further complicated because the fluid flow around the propeller is turbulent, rather than the

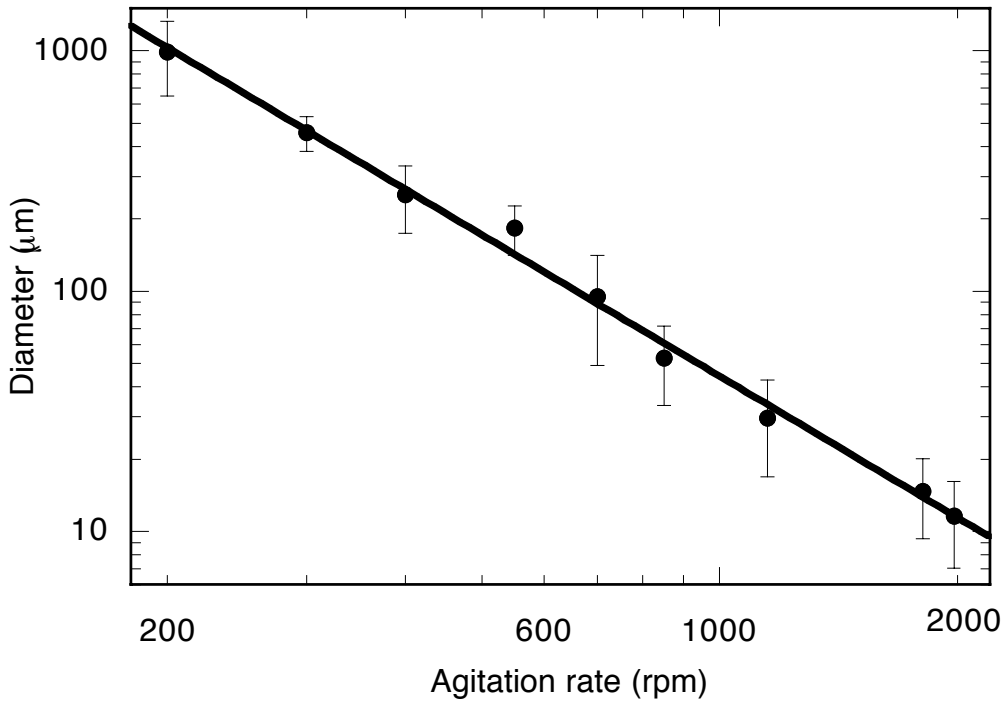

Figure 3. Mean microcapsule diameter vs. agitation rate. Size analysis was performed by optical microscopy on data sets of at least 250 measurements at each agitation rate. Error bars correspond to one standard deviation of the data. The solid line corresponds to a linear fit of the entire data on log-log scale.

laminar case analyzed by Taylor (1932). Microeddies with a range of length scales are present in the flow as described by Dobetti and Pantaleo (2002). In the region of flow away from the propeller, larger length scales dominate, leading to the major mode of the distribution shown in Figure 4. Above a characteristic length scale there are no microcapsules formed, a feature not represented by the normal curve. In the vicinity of the propeller blades many smaller microeddies exist resulting in a bias of the size distribution towards smaller length scales.

Microcapsule shell thickness

The surface morphology and shell wall thickness of microcapsules is investigated by electron microscopy. The microcapsule shell has a smooth inner membrane free of voids or inclusions, and a rough porous morphology on the outer surface, as shown in Figure 5. Excess ammonium chloride or resorcinol, addition of smaller volumes of DCPD, contaminated glassware, an unbalanced or unaligned mixer, and lower initial pH all dramatically increase the thickness of the outer, permeable layer. Park *et al*. (2001) report that the presence of both a porous and non-porous zone is a common feature of UF microcapsules.

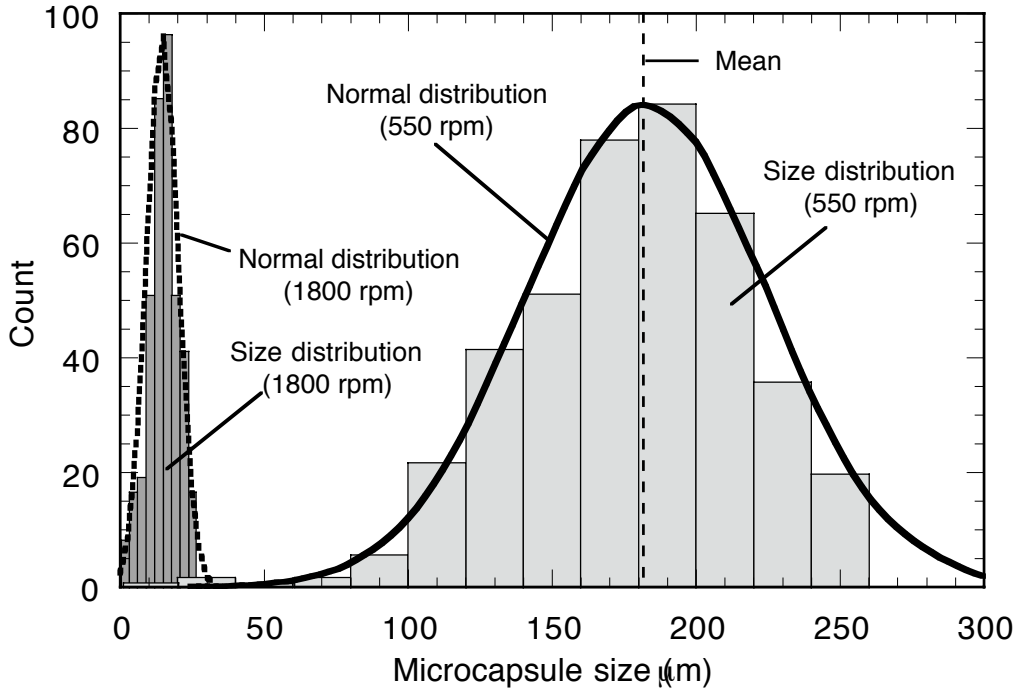

Figure 4. Microcapsule size distributions. At 550 rpm agitation rate the mean size is 183 ± 42 μm (±1 standard deviation). At 1800 rpm the mean size is 15 ± 5 μm. Standard normal distribution curves are overlaid with the data.

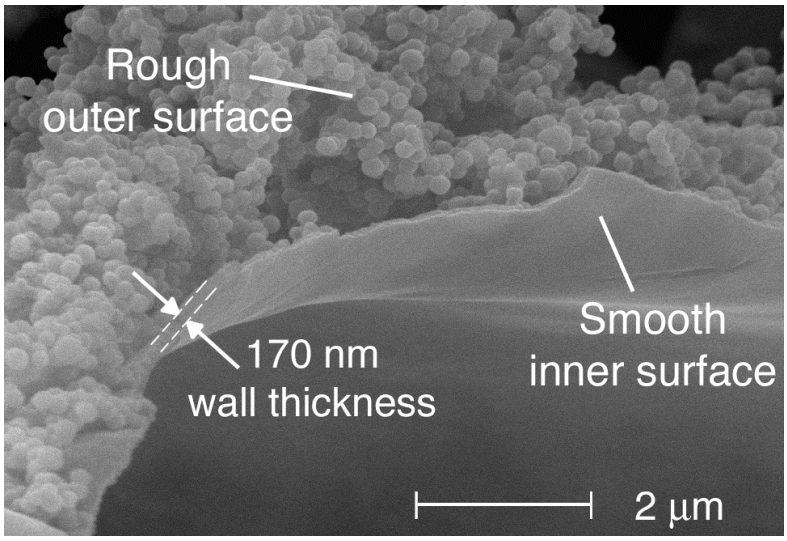

Figure 5. Microcapsule surface morphology. The rough outer surface is composed of UF nanoparticles (~150 nm) attached to the microcapsule shell.

The shell wall thickness (of the smooth nonporous inner region) is largely independent of manufacturing parameters. Shell wall thickness consistently falls between 160–220 nm over the full range of microcapsule diameters investigated. Microcapsules in this range of shell thickness are sufficiently robust to survive handling and manufacture of self-healing polymers. When embedded in an epoxy matrix the microcapsules rupture and release their content at the site of damage (Brown *et al*. 2002). The rough porous structure on the outer surface is an agglomeration of UF nanoparticles, shown in Figure 5.

Microcapsule surface morphology

The bath temperature, solution temperature, and pH were monitored during a standard microencapsulation process (Figure 6) while simultaneously removing aliquots from the emulsion bath at periodic intervals and quenching in 20 ml of cold (~15 °C) water. A sequence of aliquot images is shown along the bottom border of Figure 6. Aliquots were imaged optically with incident light with black corresponding to an optically clear solution and white indicating a milky solution.

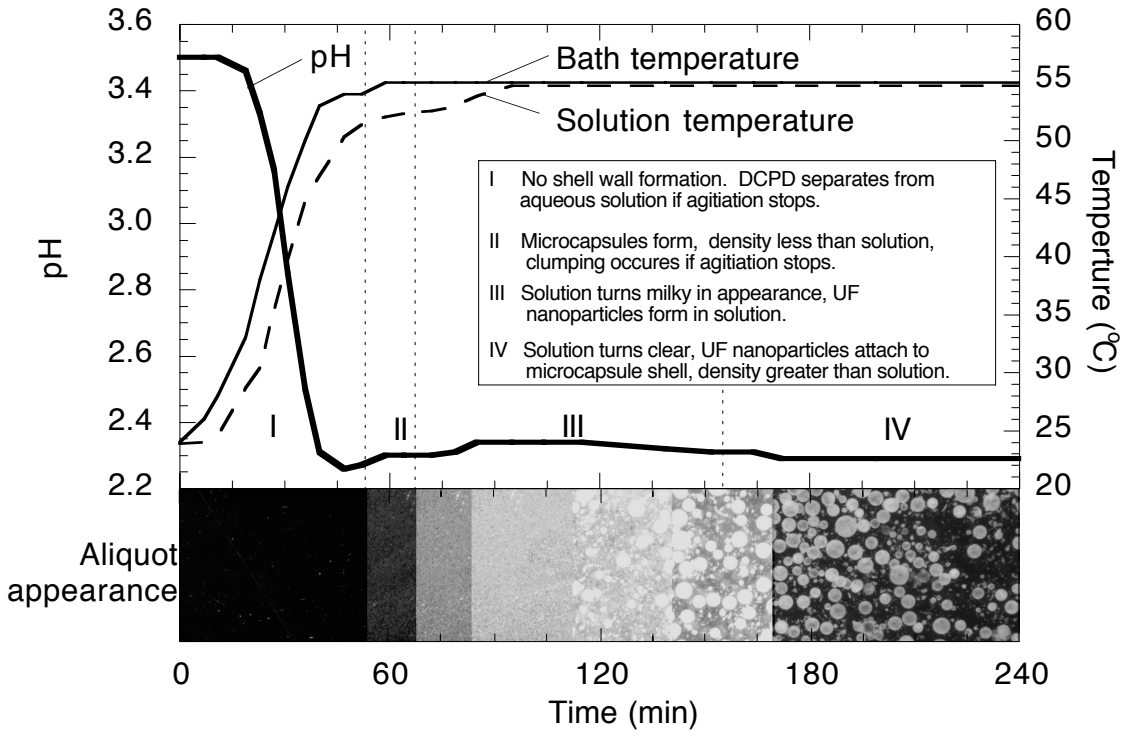

Figure 6. Temperature and pH profile during microencapsulation. Aliquot appearance was obtained by quenching in 15 °C water at periodic intervals and imaging by reflected light.

Four distinct regimes are identified. In region I (0-50 min) the DCPD emulsion appears black (clear). At low agitation rates, individual DCPD droplets are observed. The DCPD rapidly coalesces to form a distinct second phase floating above the aqueous solution if agitation is stopped. During this time period the bath temperature continuously increases to the set point, the solution temperature lags several minutes behind the bath temperature, and the pH reduces from 3.50 to about 2.35. Region II (50-70 min) is defined by the transition to a cloudy emulsion and an associated slight increase in pH. Droplets remain as distinct microcapsules if agitation is stopped. However, the microcapsules clump and are too fragile to isolate. Region III (70-160 min) shows a transition to milky white emulsion in which the temperature stabilizes and the pH peaks at about 2.45 and then steadily decreases. Separable microcapsules appear when agitation is stopped. The microcapsule shell reaches its maximum thickness and the surface morphology transitions from smooth to rough in this region, as shown in Figure 7. The milky white appearance of aliquot samples directly correlates to the development of UF nanoparticles in suspension. Electron micrographs of UF nanoparticles filtered from the solution and those found in the rough porous outer surface of microcapsules are indistinguishable. A stable pH is reached in region IV (160-240 min) and the suspension becomes clear with easily separated microcapsules.

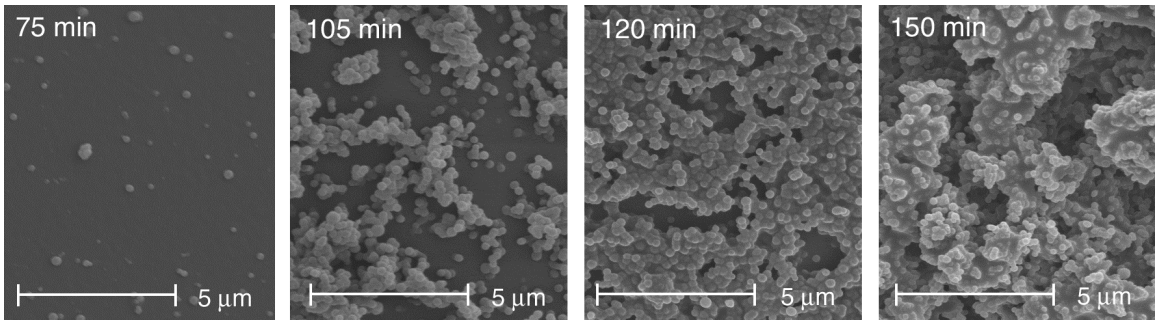

Figure 7. Microcapsule surface morphology evolution during Region III.

The onset of rough surface morphology occurs approximately 75 min into the microencapsulation reaction. To preserve the smooth surface morphology, attempts were made to end the reaction at this time. If agitation is stopped and the reaction is allowed to cool naturally under ambient conditions, the emulsion forms a single gelatinous structure and individual microcapsules cannot be obtained. If agitation is stopped and the reaction is quenched with ~15 °C water, individual smooth microcapsules are produced, but their quality is poor. The microcapsules are difficult to filter and once separated, they turn yellow over a period of 3-10 days as the DCPD diffuses through the shell.

During *in situ* polymerization the urea and formaldehyde react in the water phase to form a low molecular weight prepolymer. As the molecular weight of the prepolymer increases, it deposits at the DCPD-water interface. The UF ultimately becomes highly crosslinked and forms the microcapsule shell wall (Thies 1987). Gelation of bulk UF resin is attributed to the coalescence of a lyophobic colloidal sol (Pratt *et al*., 1985), which is known to precipitate out of solution as the molecular weight increases (Dunker *et al*., 1986). In light of this, the smooth non-porous microcapsule wall is believed to be the result of the deposition of low molecular weight prepolymer at the DCPD-water interface while the prepolymer remains soluble. The formation of UF nanoparticles is attributed to precipitation of higher molecular weight prepolymer in the aqueous solution, and their aggregation and deposition on the capsule surface results in the rough, porous outer layer of the UF shell.

The appearance of UF nanoparticles in the emulsion and their subsequent deposition on the microcapsule surface occurs during Region III after the pH has dropped dramatically from initial conditions. Since the addition phase of UF polymerization is catalyzed by either acid or base, the precipitous drop in pH leads to a rapid increase in polymerization rate. Mehdiabadi *et al*. (1998) show that as the pH decreases, the rate of increase in viscosity is accelerated dramatically. These rapid changes in viscosity at the DCPD-water interface affect the mechanics of droplet formation and suspension in shear flow. Sanghvi and Nairn (1992) conclude that interfacial surface tension was the dominant factor in controlling surface morphology of emulsion type microcapsules. Alexandridou *et al*. (2001) also report that surface morphology is dependent on functionality of the reactants and pH of the reaction solution.

Although acceptable levels of surface roughness for self-healing applications were obtained by the standard microencapsulation process, two modified processes were also investigated in an attempt to control surface morphology. First, a microencapsulation was carried out at constant pH conditions (Figure 8) by drop-wise addition of NaOH and HCl. Aliquot analysis of Region III reveals a milky white emulsion with separable microcapsules. However, the UF nanoparticles remained in suspension and did not deposit onto the microcapsule surface. The presence of suspended nanoparticles made the filtration process cumbersome and yields were low (<10%). As shown in Figure 9a, the microcapsules produced by this method possessed a smooth surface morphology, free of nanoparticle agglomeration.

Surface roughness also decreased as the agitation rate increased. For a fixed volume of encapsulated DCPD, increasing the agitation rate reduced the mean microcapsule diameter and increased the DCPD-water interfacial area. To further investigate the effect of interfacial area for a fixed size of microcapsule, the volume of DCPD added to the emulsion was increased from 60 ml to 180 ml while maintaining the

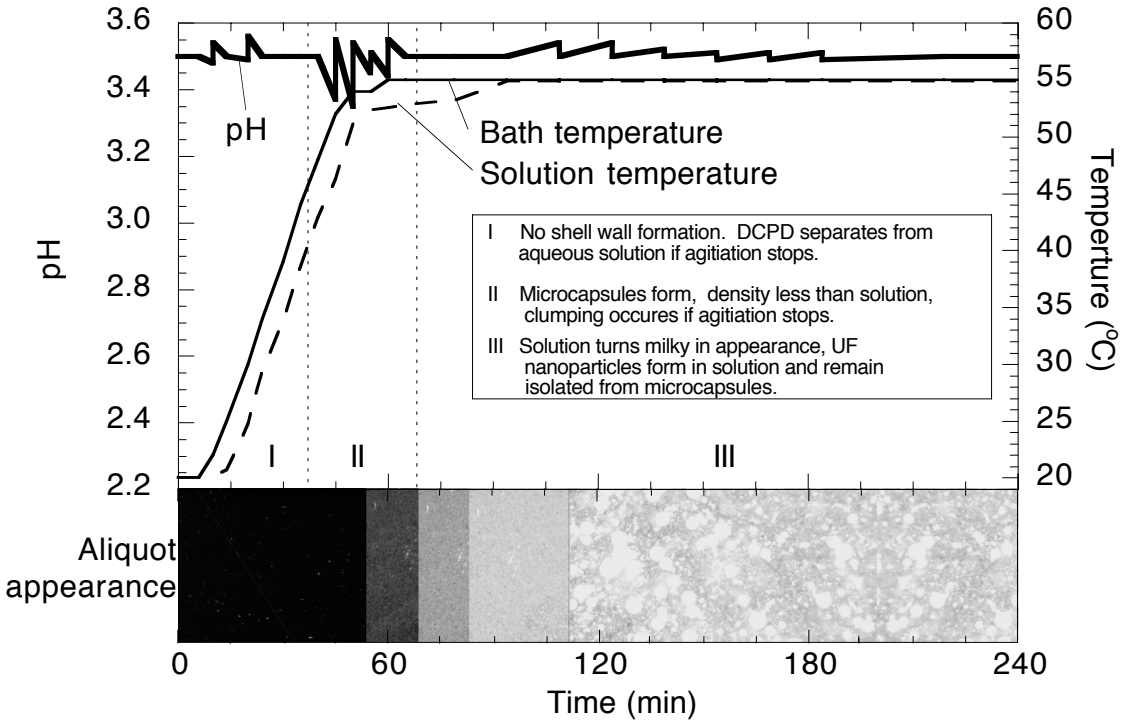

Figure 8. Temperature and pH profile during microencapsulation while maintaining constant pH conditions.

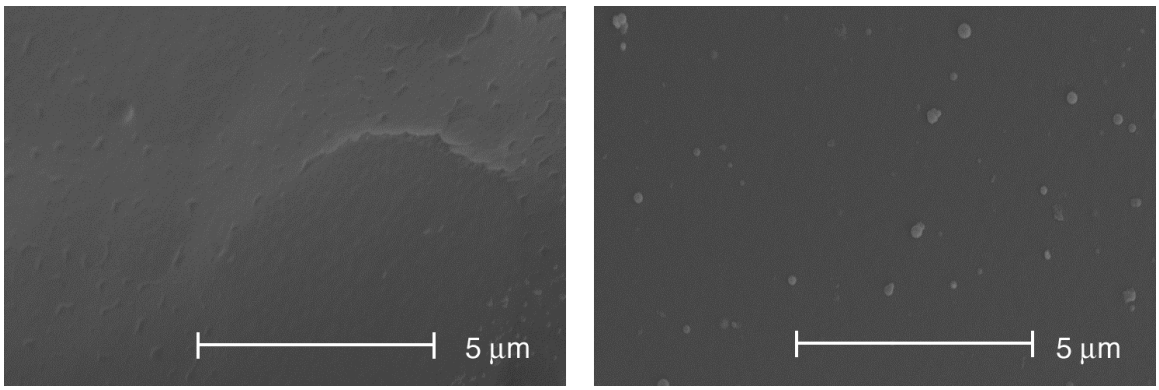

Figure 9. Surface morphology of smooth microcapsules obtained through (a) constant pH conditions and (b) increased interfacial area (180 ml DCPD). Microencapsulation at 550 rpm agitation rate (183 μm mean diameter).

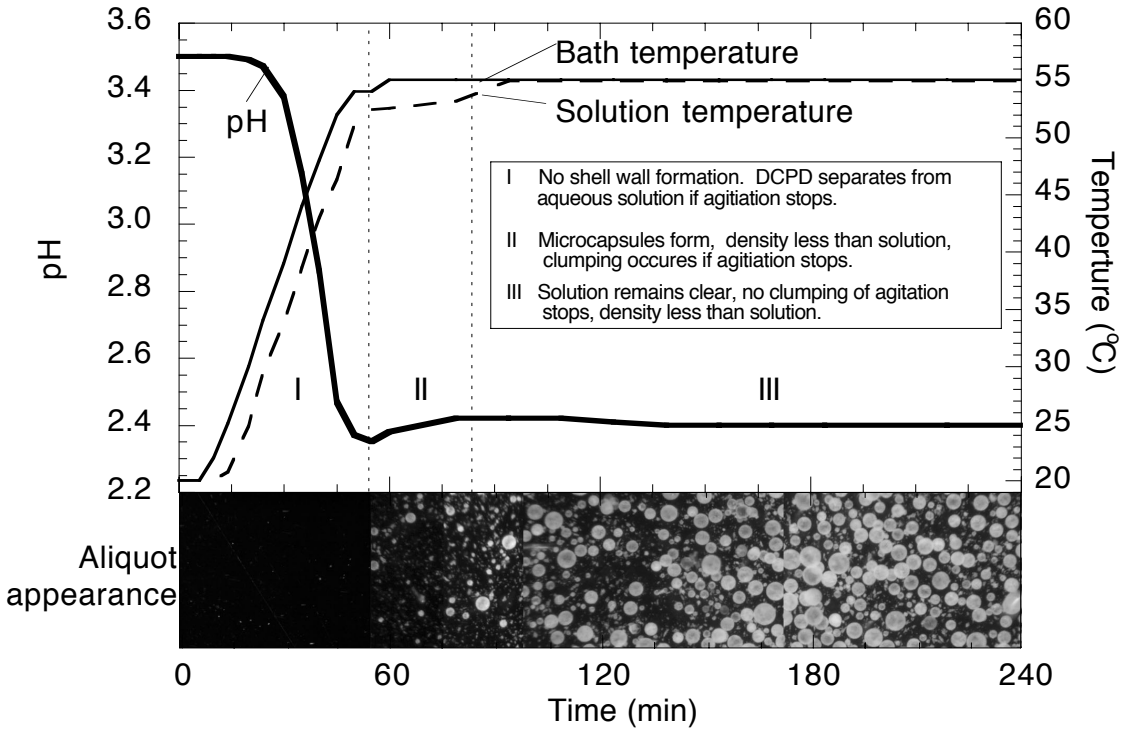

Figure 10. Temperature and pH profile during microencapsulation for increased interfacial area condition. The volume of DCPD encapsulated was increased from 60 ml to 180 ml while maintaining 550 rpm agitation rate.

same agitation rate of 550 rpm. As shown in Figure 10, the emulsion transitioned directly to a clear suspension of distinct, easily filtered microcapsules in region III. The formation of UF nanoparticles was inhibited and the resulting microcapsules had smooth surface morphology (Figure 9b). The microcapsules were free flowing, and yields were high (>85%).

Microcapsule fill content

Elemental analysis was performed on microcapsules to determine their fill content. Immediately following manufacturing and drying, microcapsules contain 83-92 wt% DCPD and 6-12 wt% UF, as measured by CHN analysis. The unidentified weight was accounted for by water absorption and UF chemical structure variation (Rammon *et al.* 1986). After 30 days exposed to ambient laboratory conditions the average fill content decreased by 2.3 wt%. When used for self-healing epoxy, microcapsules are embedded in the matrix well within this time frame. The surrounding matrix also limits further diffusion of DCPD through the microcapsule shell.

Conclusions

A process for the microencapsulation of dicyclopentadiene (DCPD) by *in situ* polymerization of urea-formaldehyde (UF) in an oil-in-water emulsion was developed to fulfill requirements for self-healing material applications. Microcapsules with average diameter in the range of 10-1000 μm were manufactured by varying the rate of agitation over the range 200-2000 rpm. As the agitation rate increased, the mean diameter decreased. Spherical microcapsules were obtained in the form of a free flowing powder, exhibiting no agglomeration and yields of the preparation were high. Microcapsule shell thickness was 160-220 nm, providing excellent storage and release properties for self-healing applications. During the microencapsulation process UF nanoparticles formed and deposited on the microcapsule surface producing a rough surface morphology. Surface roughness enhanced mechanical adhesion of the microcapsules when embedded in a polymer and improved performance in self-healing applications. The UF nanoparticles were prevented from depositing on the microcapsule surface by carrying out the reaction under constant pH conditions, but yields were low. Increasing the core-water interfacial area produced microcapsules with smooth surface morphology with high yields. Fill content was 83-92 wt% and remained high for the time period required for manufacture of self-healing polymers and polymer composites.

Acknowledgements

This material is based upon work supported by the AFOSR Aerospace and Materials Science Directorate Mechanics and Materials Program under Award No. F49620-00-1-0094, Motorola Labs, Motorola Advanced Technology Center (Schaumburg, IL), and the Beckman Institute for Advanced Science and Technology at the University of Illinois. Any opinions, findings, and conclusions or recommendations expressed in this publication are those of the authors and do not necessarily reflect the views of the AFOSR, Motorola Labs, or the Beckman Institute. The authors would also like to thank Prof. C. Thies at Washington University and Prof. J. Moore, Prof. P. Geubelle, Prof. P. Braun, S. Sriram, and S. McClennan at the University of Illinois at Urbana-Champaign for technical support and helpful discussions. Elemental analysis was performed by S. McClennan. Electron microscopy was performed in the Imaging Technology Group, Beckman Institute, of the University of Illinois at Urbana-Champaign, with the assistance of S. Robinson.

References

ALEXANDRIDOU, S. and KIPARISSIDES, C., 1994, Production of oil-containing polyterephthalamide microcapsules by interfacial polymerization - an experimental investigation of the effects of process variables on the microcapsule size distribution, *Journal of Microencapsulation*, **11**, 603-614.

ALEXANDRIDOU, S., KIPARISSIDES, C., MANGE, F., and FOISSY, A., 2001, Surface characterization of oil-containing polyterephthalamide microcapsules prepared by interfacial polymerization, *Journal of Microencapsulation*, **18**, 767-781.

ARSHADY, R., and GEORGE, M.H., 1993, Suspension, dispersion, and interfacial polycondensation - a methodological survey, *Polymer Engineering and Science*, **33**, 865-876.

BROWN, E.N., SOTTOS, N.R., and WHITE, S.R., 2002, Fracture testing of a self-healing polymer composite, *Experimental Mechanics*, **42**, 372-379.

BAXTER, G., 1974, Microencapsulation processes in modern business forms. In *Microencapsulation: Processes and Applications*, edited by J.E. Vandegaer (New York, Plenum Press).

DIETRICH, K., HERMA, H., NASTKE, R., BONATZ, E., and TEIGE, W., 1989, Amino resin microcapsules, *Acta Polymerica*, **40**, 243-251.

DOBETTI, L., and PANTALEO, V., 2002, Application of a hydrodynamic model to microencapsulation by coacervation, *Journal of Microencapsulation*, **19**, 139-151.

DUNKER, A.K., WILLIAM, E.J., RAMMON, R., FARMER, B., and JOHNS, S.J., 1986, Slightly bizarre protein chemistry: Urea-formaldehyde resin from a biochemical perspective, *Journal of Adhesion*, **19**, 153-176.

MEHDIABADI, S., NEHZAT, M.S., and BAGHERI, R., 1998, Correlating viscosity in urea-formaldehyde polymerization, *Journal of Applied Polymer Science*, **69**, 631-636.

OVEZ, B., CITAK, B., OZTEMEL, D., BALBAS, A., PEKER, S., and CAKIR, S., 1997, Variation of droplet sizes during the formation of microspheres from emulsions, *Journal of Microencapsulation*, **14**, 489-499.

PARK, S.J., SHIN, Y.S., and LEE, J.R., 2001, Preparation and characterization of microspheres containing lemon oil, *Journal of Colloid and Interface Science*, **241**, 502-508.

PRATT, T.J., WILLIAM, E.J., RAMMON, R.M. and PLAGEMANN, W.L., 1985, A novel concept on the structure of cured urea-formaldehyde resin, *Journal of Adhesion*, **17**, 275-295.

RAMMON, R.M., JOHNS, W.E., MAGNUSON, J., and DUNKER, A.K., 1986, The chemical-structure of UF resins, *Journal of Adhesion*, **19**, 115-135.

SANGHVI, S.P., and NAIRN, J.G., 1992, Effect of viscosity and interfacial-tension on particle-size of cellulose acetate trimellitate microspheres, *Journal of Microencapsulation*, **9**, 215-227.

TAN, H.S., NG, T.H., and MAHABADI, H.K., 1991, Interfacial polymerization encapsulation of a viscous pigment mix - Emulsification conditions and particle-size distribution, *Journal of Microencapsulation*, **8**, 525-536.

TAYLOR, G.I., 1932, The viscosity of a fluid containing small drops of another fluid, *Proceedings of the Royal Society*, **A138**, 41-48.

THIES, C., 1987, Microencapsulation. In *Encyclopedia of Polymer Science and Engineering*, Vol. 9, 2nd Ed., edited by H.F. Mark, N. Bikales, C.G. Overberger, G. Menges, J.I. Kroschwitz (New York, Chichester : Wiley).

THIES, C., 1996, A Survey of Microencapsulation Processes. In *Microencapsulation: Methods and Industrial Applications*, edited by S. Benita (New York, Marcel Dekker, Inc.).

WHITE, S.R., SOTTOS, N.R., GEUBELLE, P.H., MOORE, J.S., KESSLER, M.R., SRIRAM, S.R., BROWN, E.N, and VISWANATHAN, S., 2001, Autonomic healing of polymer composites, *Nature*, **409**, 794–797.

YAN, N., NI, P., and ZHANG, M., 1993, Preparation and properties of polyurea microcapsules with nonionic surfactant as emulsifier, *Journal of Microencapsulation*, **10**, 375-383.

List of Recent TAM Reports

No.	Authors	Title	Date
931	Balachandar, S., and F. M. Najjar	Optimal two-dimensional models for wake flows—*Physics of Fluids*, in press (2000)	Mar. 2000
932	Yoon, H. S., K. V. Sharp, D. F. Hill, R. J. Adrian, S. Balachandar, M. Y. Ha, and K. Kar	Integrated experimental and computational approach to simulation of flow in a stirred tank—*Chemical Engineering Sciences* **56**, 6635–6649 (2001)	Mar. 2000
933	Sakakibara, J., Hishida, K., and W. R. C. Phillips	On the vortical structure in a plane impinging jet—*Journal of Fluid Mechanics* **434**, 273–300 (2001)	Apr. 2000
934	Phillips, W. R. C.	Eulerian space–time correlations in turbulent shear flows—*Physics of Fluids* **12**, 2056–2064 (2000)	Apr. 2000
935	Hsui, A. T., and D. N. Riahi	Onset of thermal–chemical convection with crystallization within a binary fluid and its geological implications—*Geochemistry, Geophysics, Geosystems* **2**, 2000GC000075 (2001)	Apr. 2000
936	Cermelli, P., E. Fried, and S. Sellers	Configurational stress, yield, and flow in rate-independent plasticity—*Proceedings of the Royal Society of London A* **457**, 1447–1467 (2001)	Apr. 2000
937	Adrian, R. J., C. Meneveau, R. D. Moser, and J. J. Riley	Final report on 'Turbulence Measurements for Large-Eddy Simulation' workshop	Apr. 2000
938	Bagchi, P., and S. Balachandar	Linearly varying ambient flow past a sphere at finite Reynolds number—Part 1: Wake structure and forces in steady straining flow	Apr. 2000
939	Gioia, G., A. DeSimone, M. Ortiz, and A. M. Cuitiño	Folding energetics in thin-film diaphragms—*Proceedings of the Royal Society of London A* **458**, 1223–1229 (2002)	Apr. 2000
940	Chaïeb, S., and G. H. McKinley	Mixing immiscible fluids: Drainage induced cusp formation	May 2000
941	Thoroddsen, S. T., and A. Q. Shen	Granular jets—*Physics of Fluids* **13**, 4–6 (2001)	May 2000
942	Riahi, D. N.	Non-axisymmetric chimney convection in a mushy layer under a high-gravity environment—In *Centrifugal Materials Processing* (L. L. Regel and W. R. Wilcox, eds.), 295–302 (2001)	May 2000
943	Christensen, K. T., S. M. Soloff, and R. J. Adrian	PIV Sleuth: Integrated particle image velocimetry interrogation/validation software	May 2000
944	Wang, J., N. R. Sottos, and R. L. Weaver	Laser induced thin film spallation—*Experimental Mechanics* (submitted)	May 2000
945	Riahi, D. N.	Magnetohydrodynamic effects in high gravity convection during alloy solidification—In *Centrifugal Materials Processing* (L. L. Regel and W. R. Wilcox, eds.), 317–324 (2001)	June 2000
946	Gioia, G., Y. Wang, and A. M. Cuitiño	The energetics of heterogeneous deformation in open-cell solid foams—*Proceedings of the Royal Society of London A* **457**, 1079–1096 (2001)	June 2000
947	Kessler, M. R., and S. R. White	Self-activated healing of delamination damage in woven composites—*Composites A: Applied Science and Manufacturing* **32**, 683–699 (2001)	June 2000
948	Phillips, W. R. C.	On the pseudomomentum and generalized Stokes drift in a spectrum of rotational waves—*Journal of Fluid Mechanics* **430**, 209–229 (2001)	July 2000
949	Hsui, A. T., and D. N. Riahi	Does the Earth's nonuniform gravitational field affect its mantle convection?—*Physics of the Earth and Planetary Interiors* (submitted)	July 2000
950	Phillips, J. W.	Abstract Book, 20th International Congress of Theoretical and Applied Mechanics (27 August – 2 September, 2000, Chicago)	July 2000

List of Recent TAM Reports (cont'd)

No.	Authors	Title	Date
951	Vainchtein, D. L., and H. Aref	Morphological transition in compressible foam—*Physics of Fluids* **13**, 2152–2160 (2001)	July 2000
952	Chaïeb, S., E. Sato-Matsuo, and T. Tanaka	Shrinking-induced instabilities in gels	July 2000
953	Riahi, D. N., and A. T. Hsui	A theoretical investigation of high Rayleigh number convection in a nonuniform gravitational field—*International Journal of Pure and Applied Mathematics*, in press (2003)	Aug. 2000
954	Riahi, D. N.	Effects of centrifugal and Coriolis forces on a hydromagnetic chimney convection in a mushy layer—*Journal of Crystal Growth* **226**, 393–405 (2001)	Aug. 2000
955	Fried, E.	An elementary molecular-statistical basis for the Mooney and Rivlin–Saunders theories of rubber-elasticity—*Journal of the Mechanics and Physics of Solids* **50**, 571–582 (2002)	Sept. 2000
956	Phillips, W. R. C.	On an instability to Langmuir circulations and the role of Prandtl and Richardson numbers—*Journal of Fluid Mechanics* **442**, 335–358 (2001)	Sept. 2000
957	Chaïeb, S., and J. Sutin	Growth of myelin figures made of water soluble surfactant—Proceedings of the 1st Annual International IEEE–EMBS Conference on Microtechnologies in Medicine and Biology (October 2000, Lyon, France), 345–348	Oct. 2000
958	Christensen, K. T., and R. J. Adrian	Statistical evidence of hairpin vortex packets in wall turbulence—*Journal of Fluid Mechanics* **431**, 433–443 (2001)	Oct. 2000
959	Kuznetsov, I. R., and D. S. Stewart	Modeling the thermal expansion boundary layer during the combustion of energetic materials—*Combustion and Flame*, in press (2001)	Oct. 2000
960	Zhang, S., K. J. Hsia, and A. J. Pearlstein	Potential flow model of cavitation-induced interfacial fracture in a confined ductile layer—*Journal of the Mechanics and Physics of Solids*, **50**, 549–569 (2002)	Nov. 2000
961	Sharp, K. V., R. J. Adrian, J. G. Santiago, and J. I. Molho	Liquid flows in microchannels—Chapter 6 of *CRC Handbook of MEMS* (M. Gad-el-Hak, ed.) (2001)	Nov. 2000
962	Harris, J. G.	Rayleigh wave propagation in curved waveguides—*Wave Motion* **36**, 425–441 (2002)	Jan. 2001
963	Dong, F., A. T. Hsui, and D. N. Riahi	A stability analysis and some numerical computations for thermal convection with a variable buoyancy factor—*Journal of Theoretical and Applied Mechanics* **2**, 19–46 (2002)	Jan. 2001
964	Phillips, W. R. C.	Langmuir circulations beneath growing or decaying surface waves—*Journal of Fluid Mechanics* (submitted)	Jan. 2001
965	Bdzil, J. B., D. S. Stewart, and T. L. Jackson	Program burn algorithms based on detonation shock dynamics—*Journal of Computational Physics* (submitted)	Jan. 2001
966	Bagchi, P., and S. Balachandar	Linearly varying ambient flow past a sphere at finite Reynolds number: Part 2—Equation of motion—*Journal of Fluid Mechanics* (submitted)	Feb. 2001
967	Cermelli, P., and E. Fried	The evolution equation for a disclination in a nematic fluid—*Proceedings of the Royal Society A* **458**, 1–20 (2002)	Apr. 2001
968	Riahi, D. N.	Effects of rotation on convection in a porous layer during alloy solidification—Chapter 12 in *Transport Phenomena in Porous Media* (D. B. Ingham and I. Pop, eds.), 316–340 (2002)	Apr. 2001
969	Damljanovic, V., and R. L. Weaver	Elastic waves in cylindrical waveguides of arbitrary cross section—*Journal of Sound and Vibration* (submitted)	May 2001
970	Gioia, G., and A. M. Cuitiño	Two-phase densification of cohesive granular aggregates—*Physical Review Letters* **88**, 204302 (2002) (in extended form and with added co-authors S. Zheng and T. Uribe)	May 2001

List of Recent TAM Reports (cont'd)

No.	Authors	Title	Date
971	Subramanian, S. J., and P. Sofronis	Calculation of a constitutive potential for isostatic powder compaction—*International Journal of Mechanical Sciences* (submitted)	June 2001
972	Sofronis, P., and I. M. Robertson	Atomistic scale experimental observations and micromechanical/ continuum models for the effect of hydrogen on the mechanical behavior of metals—*Philosophical Magazine* (submitted)	June 2001
973	Pushkin, D. O., and H. Aref	Self-similarity theory of stationary coagulation—*Physics of Fluids* **14**, 694–703 (2002)	July 2001
974	Lian, L., and N. R. Sottos	Stress effects in ferroelectric thin films—*Journal of the Mechanics and Physics of Solids* (submitted)	Aug. 2001
975	Fried, E., and R. E. Todres	Prediction of disclinations in nematic elastomers—*Proceedings of the National Academy of Sciences* **98**, 14773–14777 (2001)	Aug. 2001
976	Fried, E., and V. A. Korchagin	Striping of nematic elastomers—*International Journal of Solids and Structures* **39**, 3451–3467 (2002)	Aug. 2001
977	Riahi, D. N.	On nonlinear convection in mushy layers: Part I. Oscillatory modes of convection—*Journal of Fluid Mechanics* **467**, 331–359 (2002)	Sept. 2001
978	Sofronis, P., I. M. Robertson, Y. Liang, D. F. Teter, and N. Aravas	Recent advances in the study of hydrogen embrittlement at the University of Illinois—Invited paper, Hydrogen–Corrosion Deformation Interactions (Sept. 16–21, 2001, Jackson Lake Lodge, Wyo.)	Sept. 2001
979	Fried, E., M. E. Gurtin, and K. Hutter	A void-based description of compaction and segregation in flowing granular materials—*Proceedings of the Royal Society of London A* (submitted)	Sept. 2001
980	Adrian, R. J., S. Balachandar, and Z.-C. Liu	Spanwise growth of vortex structure in wall turbulence—*Korean Society of Mechanical Engineers International Journal* **15**, 1741–1749 (2001)	Sept. 2001
981	Adrian, R. J.	Information and the study of turbulence and complex flow—*Japanese Society of Mechanical Engineers Journal B*, in press (2002)	Oct. 2001
982	Adrian, R. J., and Z.-C. Liu	Observation of vortex packets in direct numerical simulation of fully turbulent channel flow—*Journal of Visualization*, in press (2002)	Oct. 2001
983	Fried, E., and R. E. Todres	Disclinated states in nematic elastomers—*Journal of the Mechanics and Physics of Solids* **50**, 2691–2716 (2002)	Oct. 2001
984	Stewart, D. S.	Towards the miniaturization of explosive technology—Proceedings of the 23rd International Conference on Shock Waves (2001)	Oct. 2001
985	Kasimov, A. R., and Stewart, D. S.	Spinning instability of gaseous detonations—*Journal of Fluid Mechanics* (submitted)	Oct. 2001
986	Brown, E. N., N. R. Sottos, and S. R. White	Fracture testing of a self-healing polymer composite—*Experimental Mechanics* (submitted)	Nov. 2001
987	Phillips, W. R. C.	Langmuir circulations—*Surface Waves* (J. C. R. Hunt and S. Sajjadi, eds.), in press (2002)	Nov. 2001
988	Gioia, G., and F. A. Bombardelli	Scaling and similarity in rough channel flows—*Physical Review Letters* **88**, 014501 (2002)	Nov. 2001
989	Riahi, D. N.	On stationary and oscillatory modes of flow instabilities in a rotating porous layer during alloy solidification—*Journal of Porous Media*, in press (2002)	Nov. 2001
990	Okhuysen, B. S., and D. N. Riahi	Effect of Coriolis force on instabilities of liquid and mushy regions during alloy solidification—*Physics of Fluids* (submitted)	Dec. 2001
991	Christensen, K. T., and R. J. Adrian	Measurement of instantaneous Eulerian acceleration fields by particle-image accelerometry: Method and accuracy—*Experimental Fluids* (submitted)	Dec. 2001
992	Liu, M., and K. J. Hsia	Interfacial cracks between piezoelectric and elastic materials under in-plane electric loading—*Journal of the Mechanics and Physics of Solids*, in press (2002)	Dec. 2001
993	Panat, R. P., S. Zhang, and K. J. Hsia	Bond coat surface rumpling in thermal barrier coatings—*Acta Materialia* **51**, 239–249 (2003)	Jan. 2002

List of Recent TAM Reports (cont'd)

No.	*Authors*	*Title*	*Date*
994	Aref, H.	A transformation of the point vortex equations—*Physics of Fluids* **14**, 2395–2401 (2002)	Jan. 2002
995	Saif, M. T. A, S. Zhang, A. Haque, and K. J. Hsia	Effect of native Al_2O_3 on the elastic response of nanoscale aluminum films—*Acta Materialia* **50**, 2779–2786 (2002)	Jan. 2002
996	Fried, E., and M. E. Gurtin	A nonequilibrium theory of epitaxial growth that accounts for surface stress and surface diffusion—*Journal of the Mechanics and Physics of Solids*, in press (2002)	Jan. 2002
997	Aref, H.	The development of chaotic advection—*Physics of Fluids* **14**, 1315–1325 (2002); see also *Virtual Journal of Nanoscale Science and Technology*, 11 March 2002	Jan. 2002
998	Christensen, K. T., and R. J. Adrian	The velocity and acceleration signatures of small-scale vortices in turbulent channel flow—*Journal of Turbulence*, in press (2002)	Jan. 2002
999	Riahi, D. N.	Flow instabilities in a horizontal dendrite layer rotating about an inclined axis—*Proceedings of the Royal Society of London A* (submitted)	Feb. 2002
1000	Kessler, M. R., and S. R. White	Cure kinetics of ring-opening metathesis polymerization of dicyclopentadiene—*Journal of Polymer Science A* **40**, 2373–2383 (2002)	Feb. 2002
1001	Dolbow, J. E., E. Fried, and A. Q. Shen	Point defects in nematic gels: The case for hedgehogs—*Proceedings of the National Academy of Sciences* (submitted)	Feb. 2002
1002	Riahi, D. N.	Nonlinear steady convection in rotating mushy layers—*Journal of Fluid Mechanics*, in press (2003)	Mar. 2002
1003	Carlson, D. E., E. Fried, and S. Sellers	The totality of soft-states in a neo-classical nematic elastomer—*Proceedings of the Royal Society A* (submitted)	Mar. 2002
1004	Fried, E., and R. E. Todres	Normal-stress differences and the detection of disclinations in nematic elastomers—*Journal of Polymer Science B: Polymer Physics* **40**, 2098–2106 (2002)	June 2002
1005	Fried, E., and B. C. Roy	Gravity-induced segregation of cohesionless granular mixtures—*Lecture Notes in Mechanics*, in press (2002)	July 2002
1006	Tomkins, C. D., and R. J. Adrian	Spanwise structure and scale growth in turbulent boundary layers—*Journal of Fluid Mechanics* (submitted)	Aug. 2002
1007	Riahi, D. N.	On nonlinear convection in mushy layers: Part 2. Mixed oscillatory and stationary modes of convection—*Journal of Fluid Mechanics* (submitted)	Sept. 2002
1008	Aref, H., P. K. Newton, M. A. Stremler, T. Tokieda, and D. L. Vainchtein	Vortex crystals—*Advances in Applied Mathematics* **39**, in press (2002)	Oct. 2002
1009	Bagchi, P., and S. Balachandar	Effect of turbulence on the drag and lift of a particle—*Physics of Fluids* (submitted)	Oct. 2002
1010	Zhang, S., R. Panat, and K. J. Hsia	Influence of surface morphology on the adhesive strength of aluminum/epoxy interfaces—*Journal of Adhesion Science and Technology* (submitted)	Oct. 2002
1011	Carlson, D. E., E. Fried, and D. A. Tortorelli	On internal constraints in continuum mechanics—*Journal of Elasticity* (submitted)	Oct. 2002
1012	Boyland, P. L., M. A. Stremler, and H. Aref	Topological fluid mechanics of point vortex motions—*Physica D* **175**, 69–95 (2002)	Oct. 2002
1013	Bhattacharjee, P., and D. N. Riahi	Computational studies of the effect of rotation on convection during protein crystallization—*Journal of Crystal Growth* (submitted)	Feb. 2003
1014	Brown, E. N., M. R. Kessler, N. R. Sottos, and S. R. White	*In situ* poly(urea-formaldehyde) microencapsulation of dicyclopentadiene—*Journal of Microencapsulation* (submitted)	Feb. 2003